Scheme II

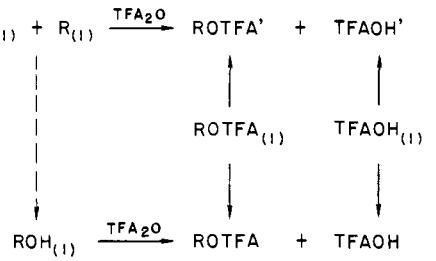

(1) $R_{(l)} + TFAOH' + TFA_2O' + S' \rightarrow ROTFA' + TFA_2O' + S'$
(2) $H_2O_{(l)} + TFAOH + TFA_2O + S \rightarrow 3TFAOH + S$
(3) $ROH_{(l)} + TFAOH + TFA_2O + S \rightarrow ROTFA + 2TFAOH + S$
(4) $ROTFA_{(l)} + TFAOH + TFA_2O + S \rightarrow ROTFA + TFAOH + TFA_2O + S$
(5) $ROTFA_{(l)} + TFAOH' + TFA_2O' + S' \rightarrow ROTFA' + TFAOH' + TFA_2O' + S'$
(6) $TFAOH_{(l)} + TFAOH + TFA_2O + S \rightarrow 2TFAOH + TFA_2O + S$
(7) $TFAOH_{(l)} + TFAOH' + TFA_2O' + S' \rightarrow 2TFAOH' + TFA_2O' + S'$
(1 + 2) $R_{(l)} + H_2O_{(l)} + TFAOH' + TFA_2O \rightarrow ROTFA' + 2TFAOH$
− 3) $R_{(l)} + H_2O_{(l)} + TFAOH' + ROTFA \rightarrow ROTFA' + TFAOH + ROH_{(l)}$
+ 4) $R_{(l)} + H_2O_{(l)} + TFAOH' + ROTFA_{(l)} \rightarrow ROTFA' + TFAOH + ROH_{(l)}$
− 5) $R_{(l)} + H_2O_{(l)} + TFAOH' \rightarrow TFAOH + ROH_{(l)}$
− 6) $R_{(l)} + H_2O_{(l)} + TFAOH' \rightarrow TFAOH_{(l)} + ROH_{(l)}$
+ 7) $R_{(l)} + H_2O_{(l)} \rightarrow ROH_{(l)}$

and saturated aqueous $NaHCO_3$. The organic layer was washed with $NaHCO_3$ until the aqueous layer was basic, and then dried over $MgSO_4$ and filtered. This procedure was repeated for samples at 100 and 150 °C.

The ratio of 2-hexyl trifluoroacetate to 3-hexyl trifluoroacetate was measured using an F&M 700 gas chromatograph equipped with a 35 ft × $^1/_8$ in. didecyl phthalate on 70/80 ABS column. Relative response factors were determined by preparing a known sample of 66.5% 2-hexyl trifluoroacetate and 33.5% 3-hexyl trifluoroacetate. The peak areas were integrated with a Varian CDS-111 digital integrator. The ratio of the peaks were measured with a precision of approximately 1% as indicated in Table I.

Product Ratio from Trifluoroacetolysis. A drop of the appropriate hexene was added to an NMR tube containing the standard calorimetry solvent (0.002 M TFMSA). After 10 min its spectrum was measured using a Brucker HX270 spectrometer with homonuclear gated decoupling to supress the solvent acid peak. Four transients were collected with a 10-s pulse delay. Three multiplets were used in the analysis: (a) δ 1.65, (b) δ = 1.4, and (c), δ 1.0. Standard samples were prepared with 2-hexyl trifluoroacetate/3-hexyl trifluoroacetate ratios of 1.34, 0.981, and 0.546 in solvent without TFMSA so that they would not isomerize. The peaks were digitally integrated and the ratios of their areas determined. The peak area ratio a:c was invariant with composition. By interpolation of the a:b and b:c area ratios the composition for each sample could be determined. Each sample was measured in duplicate, and all values were averaged to give those in Table III. The number of moles needed to convert the trifluoroacetate ratio to the equilibrium value of 1.68 was then multiplied by 172 cal/mol (from Table I) to give the correction factor for conversion of the enthalpy of reaction to formation of the equilibrium mixture.

Derivation of Enthalpy of Hydration. The enthalpy of hydration was calculated using the equations (in Scheme II) which take into account the differences in the reaction media used in the reactions of the alkenes and the alcohols. In the equations, R is an alkene, ROTFA is an equilibrium mixture of the trifluoroacetates, S is the reaction solvent minus 1 equiv of TFAOH and 1 equiv of TFA_2O, (l) indicates in the pure liquid state, and ′ indicates in the presence of strong acid. A schematic diagram of the cycle used to derive the heat of hydration is shown in the Scheme. Following that is a rigorous derivation. The enthalpy of each of the reactions 1-7 was determined, and combined to give the enthalpy of hydration.

Acknowledgment. This investigation was supported by the Office of Basic Energy Science, Department of Energy.

Study of Increasingly Crowded Phenylethanes by ^{13}C NMR Spectroscopy and Molecular Mechanics Calculations

Michael I. Watkins and George A. Olah*

Contribution from the Hydrocarbon Research Institute and Department of Chemistry, University of Southern California, Los Angeles, California 90007. *Received October 23, 1980*

Abstract: An approach which characterizes the effect of nonbonded interactions on ^{13}C NMR shifts has been developed and applied to a complete series of phenylethanes. Force field calculations using Warshel's QCFF/PI + MCA program have been performed on the compounds to evaluate the nonbonded force on each atom used in the multiple regression analysis. X-ray crystal structure derived geometries reported in the literature have been used to compare with those obtained through calculation. The results show (1) experimental evidence for the polarization of electrons induced by nonbonded interactions, (2) the importance of steric interactions for all positions in a molecule, and (3) previously unobserved deshielding of the NMR signal of carbon due to steric compression of its bonds.

For many years[1] chemists have been keenly interested in studying the consequences of steric interactions in molecules. When two nonbonded atoms come to within the sum of their van der Waals radii of each other, they repulse one another. These atoms will in turn distort from their ideal geometry in an optimum way so as to reduce this repulsion without sacrificing too much in the way of bonding energy. Ethane substituted by phenyl groups has been a focal point for this field of interest[2] which began when Gomberg in 1900[3] proposed that "hexaphenylethane" dissociated readily to give the triphenylmethyl radical due to the large degree of strain placed on the ethane C–C bond. More recent investigators have utilized molecular mechanics,[4] X-ray structure de-

(1) For a recent review see: (a) Tidwell, T. T. *Tetrahedron* **1978**, *34*, 1855-1868. (b) Forster, H.; Vogtle, F. *Angew. Chem.* **1977**, *89*, 443-455. (c) Liebman, J. F.; Greenberg, A. *Chem. Rev.* **1976**, *76*, 311-365. (d) Voronenkov, V. V.; Osokin, Y. G. *Russ. Chem. Rev.* (*Engl. Transl.*) **1972**, *41*, 616-629.

(2) (a) Lankamp, H.; Nauta, W. T.; MacLean, C. *Tetrahedron Lett.* **1968**, 249-254. (b) McBride, J. M. *Tetrahedron* **1974**, *30*, 2009-2022.

(3) Gomberg, M. *J. Am. Chem. Soc.* **1900**, *22*, 757-771.

0002-7863/81/1503-6566$01.25/0

Table I. ^{13}C Chemical Shifts[a] of Phenylethanes

compd	no. of phenyls[b] C(1) M	C(1) N	C(2) M	C(2) N	α C_1	α C_2	ipso C_3	ipso C_7	ortho C_4	ortho C_8	meta C_5	meta C_9	para C_6	para C_{10}
ethane[c]	0	0	0	0	6.8	6.8								
ethylbenzene	1	0	0	1	30.0 (124)[d]	16.6 (126)	145.3		128.9 (159)		129.4 (156)		126.7 (160)	
1,2-diphenylethane	1	1	1	1	39.0 (127)	39.0 (127)	142.8	142.8	129.5	129.5	129.4 (159)	129.4 (159)	127.0 (160)	127.0 (160)
1,1-diphenylethane	2	0	0	2	45.9 (125)	22.9 (127)	147.5		128.7 (159)		129.4 (157)		127.1 (161)	
1,1,2-triphenylethane	2	1	1	2	54.2 (127)	43.2 (128)	145.6	141.3	129.1 (157)	130.1 (157)	129.1 (159)	129.4 (159)	127.2 (160)	126.9 (160)
1,1,1-triphenylethane	3	0	0	3	53.6	31.6 (128)	150.1		129.8 (158)		128.9 (159)		127.0 (160)	
1,1,1,2-tetraphenylethane	3	1	1	3	59.6	47.4 (128)	147.7	139.5	130.8 (157)	132.2 (158)	128.6 (159)	128.4 (160)	126.9 (160)	126.9 (160)
1,1,2,2-tetraphenylethane	2	2	2	2	57.4 (131)	57.4 (131)	144.5	144.5	129.6 (156)	129.6 (156)	129.2 (160)	129.2 (160)	126.9 (160)	126.9 (160)
1,1,1,2,2-pentaphenylethane	3	2	2	3	63.7	60.4 (127)	146.8	144.1	132.8 (156)	132.5 (156)	128.1 (160)	128.5 (160)	127.0 (160)	127.0 (160)

[a] $\delta(^{13}C)$, parts per million from external capillary Me_4Si. [b] Relative to the carbon being considered (vide infra). [c] Reference 10. [d] The numbers in parentheses are $J(C-H)$ in hertz.

terminations,[5] dipole moment measurements,[6] and infrared and Raman spectroscopy,[7] as well as nuclear magnetic resonance[8] as methods of probing the forces at work in these compounds.

One of the first properties recognized by the early pioneers of ^{13}C NMR spectroscopy was the observation of a regular and uniform change of the ^{13}C NMR shift in hydrocarbons upon substitution of hydrogen by a functional group.[9] In Proulx and Smith's ^{13}C NMR investigation[8n] into the present class of compounds only a qualitative pattern emerged in the shielding of the α- and ipso-carbons with increasing phenyl substitution. There have been many other examples reported in the literature where an additivity treatment did not accurately account for the observed shifts.[10] One of the reasons is well-known to be steric in origin but has eluded any generalized treatment. In 1967 Grant and Cheney[11,12] formulated the basic theory which has been used since then for describing the basis of the γ effect[13] in ^{13}C NMR spectroscopy. They attributed the upfield shift of the carbon γ to the site of substitution to an "induced polarization of charge along the $H^{13}C$ bond". To quantify the effect, the authors postulated a linear relationship between the γ ^{13}C substituent parameter and the component of steric force on the hydrogens directed along the carbon's C–H bonds. From their NMR data on methylcyclohexane and three conformations of *o*-xylene and with the assumption of an ideal geometry, they obtained a slope of 1.30×10^5 ppm/dyne [0.903 ppm/(kcal/Å)]. Since then Schneider et al.[14] have utilized Allinger's MM1 force field program[15] for calculating the geometry of their compounds and the Warshel–Lifson force field[16] for evaluating the nonbonded steric force along the C–H bonds. Their plot of the γ-substituent parameter vs. "total steric force" for some cyclic alkanes yielded a value of 2.0×10^4 ppm/dyne [0.139 ppm/(kcal/Å)] for the reaction of the ^{13}C shift to nonbonded interactions. While this approach has been generally accepted in the literature, it has not been without some criticism.[17] A brief summary of these criticisms is as follows: (1) sterically induced polarization of electrons should not be confined to C–H bonds exclusively; (2) steric effects have also been observed where the perturbing atom is not hydrogen; (3) similar effects should be observed for all positions in a molecule; and (4) ab initio calculations have shown that the nature and conformational relationship of the intervening bonds and atoms are as important as the nonbonded H···H interactions of the methyl groups.

(4) (a) Hounshell, W. D.; Dougherty, D. A.; Hummel, J. P.; Mislow, K. *J. Am. Chem. Soc.* **1977**, *99*, 1916–1924. (b) Dougherty, D. A.; Mislow, K. *Ibid.* **1979**, *101*, 1401–1405.

(5) (a) Allen, H. C.; Plyler, E. K. *J. Chem. Phys.* **1959**, *31*, 1062–1065. (b) Cruickshank, D. W. J. *Acta Crystallogr.* **1949**, *2*, 65–82. (c) Destro, R.; Pilati, T.; Simonetta, M. *Acta Crystallogr. Sect. B* **1980**, *B36*, 2495–2497. (d) Destro, R.; Pilati, T.; Simonetta, M. *Ibid.* **1980**, *B36*, 2497–2500. (e) Ardebili, M. H. P.; Dougherty, D. A.; Mislow, K.; Schwartz, L. H.; White, J. G. *J. Am. Chem. Soc.* **1978**, *100*, 7994–7997. (f) Destro, R.; Pilati, T.; Simonetta, M. *Ibid.* **1978**, *100*, 6507–6509.

(6) (a) Burchill, P. J. M.; Thorne, N. *J. Chem. Soc. C* **1968**, 696–700. (b) Chiu, K. K.; Huang, H. H. *J. Chem. Soc. B* **1970**, 1142–1146.

(7) (a) Harrah, L. A.; Ryan, M. T.; Tamborski, C. *Spectrochim. Acta* **1962**, *18*, 21–37. (b) Chen, S. P.; Huang, H. H. *J. Chem. Soc., Perkin Trans. 2*, **1972**, 1301–1304.

(8) (a) Reynolds, W. F.; Kohler, R. H.; Hamer, G. K. *Tetrahedron Lett.* **1976**, 4671–4674. (b) Anderson, J. E.; Doecke, C. W.; Pearson, H.; Rawson, D. I. *J. Chem. Soc., Perkin Trans. 2* **1978**, 974–978. (c) Schraml, J.; Chvalovsky, V.; Magi, M.; Lippmaa, E.; Calas, R.; Dunogues, J.; Bourgeois, P. *J. Organomet. Chem.* **1976**, *120*, 41–47. (d) Staab, H. A.; Rao, K. S.; Brunner, H. *Chem. Ber.* **1971**, *104*, 2634–2636. (e) Wittig, G.; Schoch, W. *Ann. Chem.* **1971**, *749*, 38–48. (f) Hook, S. C. W. *Tetrahedron Lett.* **1975**, 3321–3322. (g) Schwartz, L. H.; Koukotas, C.; Chen-Shek, Yu *J. Am. Chem. Soc.* **1977**, *99*, 7710–7711. (h) Finocchiaro, P.; Gust, D.; Hounshell, W. D.; Hummel, J. P.; Maravigna, P.; Mislow, K. *Ibid.* **1976**, *98*, 4945–4952. (i) Finocchiaro, P.; Hounshell, W. D.; Mislow, K. *Ibid.* **1976**, *98*, 4952–4963. (j) Llort, F. M.; Mislow, K.; Wooten, J. B.; Beyerlein, A. L.; Savitsky, G. B.; Jocobus, J. *Ibid.* **1979**, *101*, 292–295. (k) Skinner, K. J.; Hochster, H. S.; McBride, J. M. *Ibid.* **1974**, *96*, 4301–4306. (l) Baas, J. M. A.; van der Toorn, J. M.; Wepster, B. M. *Recl. Trav. Chim. Pays-Bas* **1974**, *93*, 133–135. (m) Hansen, P. E.; Poulsen, O. K.; Berg, A. *Org. Magn. Reson.* **1976**, *8*, 632–637. (n) Proulx, T. W.; Smith, W. B. *J. Magn. Reson.* **1976**, *23*, 477–480.

(9) (a) Spiesecke, H.; Schneider, W. G. *J. Chem. Phys.* **1961**, *35*, 722–730. (b) Paul, E. G.; Grant, D. M. *J. Am. Chem. Soc.* **1963**, *85*, 1701–1702. (c) Grant, D. M.; Paul, E. G. *Ibid.* **1964**, *86*, 2984–2990. (d) Savitsky, G. B.; Namikawa, K. *J. Phys. Chem.* **1964**, *68*, 1956–1961.

(10) Stothers, J. B. "Carbon-13 Spectroscopy"; Academic Press: New York, 1972; pp 55–60.

(11) Grant, D. M.; Cheney, B. V. *J. Am. Chem. Soc.* **1967**, *89*, 5315–5318.

(12) Cheney, B. V.; Grant, D. M. *J. Am. Chem. Soc.* **1967**, *89*, 5319–5327.

(13) The term "γ effect" was first introduced by Grant and Paul (see ref 9c) and referred to the upfield shift of the carbon three bonds away from the site of substitution; see also ref 10, p 404.

(14) (a) Schneider, H. J.; Weigand, E. F.; Gschwendtner, W. *J. Am. Chem. Soc.* **1977**, *99*, 8362–8363. (b) Schneider, H. J.; Gschwendtner, W.; Weigand, E. F. *Ibid.* **1979**, *101*, 7195–7198.

(15) For a review see: Allinger, N. L. *Adv. Phys. Org. Chem.* **1976**, *13*, 1–82.

(16) Warshel, A.; Lifson, S. *J. Chem. Phys.* **1970**, *53*, 582–594.

(17) (a) Lippmaa, E.; Perk, T.; Anderson, K.; Rappe, C. *Org. Magn. Reson.* **1970**, *2*, 109–121. (b) Roberts, J. D.; Weigert, F. J.; Kroschwitz, J. I.; Reich, H. J. *J. Am. Chem. Soc.* **1970**, *92*, 1338–1347. (c) Stothers, J. B.; Tan, C. T.; Teo, K. C. *J. Magn. Reson.* **1975**, *20*, 570–574. (d) Lippmaa, E.; Penk, T.; Belikova, N. A.; Bobyleva, A. A.; Kalinichenko, A. N.; Ordubadi, M. D.; Plate, A. F. *Org. Magn. Reson.* **1976**, *8*, 74–78. (e) Ayer, W. A.; Browne, L. M.; Fung, S.; Stothers, J. B. *Can. J. Chem.* **1976**, *54*, 3272–3275. (f) Stothers, J. B.; Tan, C. T. *Ibid.* **1976**, *54*, 917–925. (g) Beierbeck, H.; Saunders, J. K. *Ibid.* **1976**, *54*, 2985–2995. (h) Grutzner, J. B.; Jautelat, M.; Dence, J. B.; Smith, R. A.; Roberts, J. D. *J. Am. Chem. Soc.* **1970**, *92*, 7107–7120. (i) Seidman, K.; Maciel, G. E. *Ibid.* **1977**, *99*, 659–671. (j) Gorenstein, D. O. *Ibid.* **1977**, *99*, 2254–2258.

Table II. Calculated Geometry and ^{13}C NMR Shifts of α-Carbons (C_1, C_2) of Phenylethanes

compd	A	B	B'	C	D	D'	E	E'	F	F'	G	G'	H	I	I'
C-H (found)[g]										1.006		1.002			0.994
C-H (calcd)	1.102	1.113	1.102	1.112	1.122	1.101	1.123	1.111		1.100		1.110	1.121		1.129
C-C (found)	1.534[a]			1.510[b]					1.553[c]	1.553	1.567[d]	1.567	1.540[e]	1.606[f]	1.606
C-C (calcd)	1.539	1.533	1.533	1.534	1.544	1.544	1.534	1.534	1.562	1.562	1.553	1.553	1.545	1.561	1.561
C-Ph (found)				1.524					1.538		1.544	1.514	1.519	1.552	1.534
C-Ph (calcd)		1.489		1.490	1.490	1.494	1.496	1.491	1.504		1.510	1.490	1.512	1.522	1.509
H-C-C (found)										110.6		108.0			103
H-C-C (calcd)	110.2	107.8	110.5	109.1	106.2	110.8	106.6	109.8		111.0		109.1	107.0		103.9
Ph-C-C (found)				112.1					109.0		109.2	115.9	113.5	110.3	116.0
Ph-C-C (calcd)		115.1		112.1	110.1		112.3	111.7	107.2		108.9	115.5	114.1	110.6	117.1
H-C-H (found)										108.3		106.6			
H-C-H (calcd)	109.8	106.6	108.4	107.0		108.1	106.2			107.9		105.1			
H-C-Ph (found)												109.0			105.8
H-C-Ph (calcd)		109.6		109.7	111.3		108.3	109.6				108.7	107.2		104.2
Ph-C-Ph (found)									109.9		109.8		109.7	108.7	109.2
Ph-C-Ph (calcd)					113.3		108.7		111.6		110.0		107.0	108.3	108.6
dihedral angle (found)				60.0					63.68	63.68	61.34	61.34	62.00	62.17	62.17
dihedral angle (calcd)	60.01	60.57	60.57	61.10	62.63	62.63	64.49	64.49	65.02	65.02	61.99	61.99	60.02	60.29	60.29
C-H force[h]	0.310	0.701	−0.72	2.337	0.704	−1.57	1.628	2.895		−3.09		2.325	2.432		0.013
C-C force	0.000	2.226	2.226	3.413	4.940	4.940	4.590	4.590	10.23	10.23	7.863	7.863	4.781	6.309	6.309
C-Ph force		−7.06		−12.2	−4.39		−4.60	−15.1	−1.28		−0.14	−15.2	−5.24	−0.01	−4.97
δ(^{13}C)(calcd)	8.8	30.1	16.3	36.7	46.8	22.9	51.6	43.1	55.4	30.6	57.9	48.1	57.1	63.4	63.6
std dev	1.42	1.01	1.04	0.90	1.28	1.03	0.88	1.12	1.60	1.70	1.21	1.50	0.93	14.8	1.29

[a] Reference 5a. [b] Reference 5b. [c] Reference 5c. [d] Reference 5d. [e] Reference 5e. [f] Reference 5f. [g] Distances are in angstroms. [h] Average force per bond in kcal/Å.

In the present investigation we have examined the whole series of phenylethanes by making use of ^{13}C nuclear magnetic resonance, Warshel's QCFF/PI + MCA molecular mechanics program and the X-ray crystal structures obtained independently, as part of a cooperative effort, by M. Simonetta along with others reported in the literature. By these means we have been able to extend the Grant–Cheney treatment to all positions and bonds of the molecule by applying additivity relationships to account for any substituent-induced electronic effect and by calculating the contractive or protractive force along the bonds of each atom to quantify the steric effects of the substituents. As a means of checking the trends in the molecular mechanics calculations upon which our correlations of force and ^{13}C NMR shift are based, we have compared qualitatively the geometry obtained from the QCFF/PI + MCA program[18] with the experimentally determined X-ray crystal structures.

Results

Along with the ^{13}C NMR shifts and ^{13}C–^{1}H coupling constants presented in Table I are the substituent parameters, M and N, thus for C_1, C_3, C_4, C_5, and C_6, M and N are the number of phenyls attached to C_1 and C_2, respectively, while for C_2, C_7, C_8, C_9, and C_{10}, M and N are the number of phenyls attached to C_2 and C_1, respectively. The assignment of the ^{13}C shifts was, although frequently involved, without exception unambiguous. The following properties were the criteria used for making them. α-Carbons: (a) because of their sp^3 hybridization, these peaks appear shielded (upfield) from the aromatic region; (b) the proton-coupled spectrum of these carbons showed the number of attached hydrogens. Ipso-carbons: (a) these peaks appear deshielded (downfield) from the other aromatic carbons; (b) the peaks appear as singlets in the off-resonance spectrum; (c) their relative heights distinguished them as belonging to either the primed or unprimed half of the molecule (i.e., since the ipso-carbons belonging to each half of the compounds studied are equivalent at room temperature[19]). Para-carbons: (a) always appeared near to δ(^{13}C) 127.0, which is farther upfield from ipso, ortho, and meta; (b) when more than one para-carbon is present, their relative intensity determined which portion of the molecule they belonged to; (c) these peaks appear as a doublet of triplets in the H-coupled spectra. Ortho- and meta-carbons: (a) these are differentiated by their long-range coupling pattern, the ortho peaks appear as a doublet of triplets or quartets and the meta carbons as a doublet of doublets; (b) their relative heights is the only additional information needed to make the final assignment. As is mentioned in the Experimental Section the spectras were recorded on a Varian Associates XL-200 NMR spectrometer with a super-conducting magnet operating at 50.32 MHz for ^{13}C. At this higher field with its attendent increased resolution we were able to remove the ambiguities in the assignments of ortho- and meta-carbons for certain compounds reported previously.[8n] Thus with increasing phenyl substitution: α-carbons are deshielded, ipso-carbons are deshielded as "M" increases and shielded as "N" increases, ortho carbons are deshielded, and meta carbons are shielded. While there are trends in the data, the changes are clearly not as regular as would be expected if they were caused solely by the substituent. Consider for the moment the effect of α substitution: C_1 of ethylbenzene is deshielded by 15.9 ppm upon addition of a phenyl ring while for 1,1,2,2-tetraphenylethane C_1 is deshielded by only 6.3 ppm. These "δ" values should be equal if an additivity treatment were valid. The same discrepancies are even more apparent for other positions where the "substituent effect" is less pronounced, the cause of which is the subject of this paper.

The geometric data are presented in such a way as to simplify their examination, which utilizes the symmetry of this class of compounds and the fact that ^{13}C NMR distinguishes only certain electronically different nuclei. Each compound is designated by a letter defined in Figure 1. The letter unprimed represents the C_1 portion of the molecule (the most substituted half) and the letter primed the C_2 portion (the least substituted half of the molecule). For instance in 1,1,2-triphenylethane the properties of the ipso-carbons (C_3) of the two phenyl rings attached to C_1 are under column E and the parameters describing the ipso-carbon (C_7) of the phenyl ring attached to carbon 2 are under column E′. Thus in Tables II–VI the bond distances and angles and the bond forces have been averaged for corresponding parts for this series of phenylethanes. The fully relaxed geometries of the studied phenylethanes were calculated by using the QCFF/PI + MCA program[18] without any reparameterization. The bond lengths and angles of all atoms and the torsional angles of the phenyl rings and the central ethane linkage were allowed to change during 40 steepest-descent and 4 Newton-Rhapson convergent minimization

(18) (a) Warshel, A. "Semiempirical Methods of Electronic Structure Calculation, Part A"; Segal, G. A., Ed.; Plenum Press: New York, 1977; pp 133–171. (b) Warshel, A. *Comput. Chem.* **1977**, *1*, 195–202.

(19) The only temperature dependence observed in this series of compounds was for pentaphenylethane where the ipso's of the C_1 portion of the molecule split into two peaks of relative intensity 2:1 ($\Delta G^* = 9.89$ kcal/mol, coalescence temperature = −57 °C at 25.16 MHz).

Table III. Calculated Geometry and ^{13}C NMR Shifts of Ipso-Carbons (C_3, C_7) of Phenylethanes

compd	B	C	D	E	E'	F	G	G'	H	I	I'
C(α)-C(i) (found)[a]		1.524[b]				1.538[c]	1.544[c]	1.514	1.519[d]	1.552[f]	1.534
C(α)-C(i) (calcd)	1.489	1.490	1.494	1.496	1.491	1.504	1.510	1.490	1.512	1.522	1.509
C(i)-Co) (found)		1.374				1.387	1.392	1.386		1.391	1.392
C(i)-C(o) (calcd)	1.415	1.413	1.416	1.415	1.412	1.419	1.419	1.413	1.419	1.423	1.420
C(α)-C(i)-C(o) (found)		120.4				121.4	121.3	121.1		121.4	121
C(α)-C(i)-C(o) (calcd)	120.8	120.6	120.8	120.7	120.5	121.2	121.3	120.6	121.3	121.8	121.5
C(o)-C(i)-C'(o) (found)		119.3				117.2	117.2	117.8		116.9	116.7
C(o)-C(i)-C'(o) (calcd)	118.5	118.8	118.3	118.5	119.0	117.5	117.2	118.8	117.2	116.3	116.9
ring twist		−72.7				−40.9	89.66	−73.8	−72.5	−75.5	−49.6
angle (found)		72.74				−39.24	40.23		25.7	−1.67	−82.8
						53.94	−6.28		23.4	48.11	
									−69.7		
ring twist	−5.77	−80.8	−32.6	63.13	−78.7	−41.6	88.45	−76.3	−37.8	−51.8	50.01
angle (calcd)		−3.24	59.25	−11.6		−39.1	40.64		57.04	−46.8	−60.5
						52.28	−5.42		45.92	53.39	
									−56.1		
force $C(sp^3)$-$C(sp^2)$[g]	−7.06	−12.2	−4.39	−4.60	−15.1	−1.28	−0.14	−15.2	−5.24	−0.01	−4.97
force $C(sp^2)$-$C(sp^2)$	11.67	11.36	11.33	10.91	10.34	11.81	11.01	9.271	12.02	12.38	11.11
$\delta(^{13}C)$(calcd)	145.3	143.1	147.3	145.9	141.1	149.5	148.2	139.7	144.7	147.2	143.3
std dev	0.45	0.35	0.28	0.27	0.37	0.41	0.37	0.44	0.32	0.39	0.39

[a] Distances are in angstroms. [b] Reference 5b. [c] Reference 5c. [d] Reference 5d. [f] Reference 5f. [g] Average force per bond in kcal/Å.

Table IV. Calculated Geometry and ^{13}C NMR Shifts of Ortho-Carbons (C_4, C_8) of Phenylethanes

compd	B	C	D	E	E'	F	G	G'	H	I	I'
C(o)-C(i) (found)[a]		1.374[b]				1.387[c]	1.392[d]	1.386		1.391[e]	1.392
C(o)-C(i) (calcd)	1.415	1.413	1.416	1.415	1.412	1.419	1.419	1.413	1.419	1.423	1.420
C(m)-C(o) (found)		1.390				1.383	1.386	1.386		1.385	1.386
C(m)-C(o) (calcd)	1.406	1.405	1.405	1.405	1.405	1.405	1.405	1.405	1.405	1.405	1.405
C(o)-H (found)						0.984	0.992	1.013		0.975	0.977
C(o)-H (calcd)	1.083	1.083	1.083	1.083	1.083	1.082	1.082	1.082	1.080	1.080	1.081
C(i)-C(o)-C(m) (found)		120.5				121.2	121.3	121.0		121.5	121.6
C(i)-C(o)-C(m) (calcd)	120.7	120.5	120.8	120.7	120.4	121.2	121.3	120.5	121.4	121.8	121.5
C(i)-C(o)-H (found)						119.3	119.8	118.7		119.7	118.4
C(i)-C(o)-H (calcd)	120.7	120.5	120.7	120.6	120.5	121.0	121.1	120.7	121.5	121.8	121.8
C(m)-C(o)-H (found)						119.5	118.9	120.4		118.7	120.0
C(m)-C(o)-H (calcd)	118.6	118.9	118.7	119.0	119.1	117.8	117.6	118.8	119.4	116.4	116.7
force $C(sp^2)$-H[f]	−7.82	−8.26	−7.42	−7.70	−8.55	−6.22	−5.52	−9.15	−8.44	−6.63	−9.05
force $C(sp^2)$-$C(sp^2)$	8.571	8.843	7.424	7.495	8.504	5.728	4.818	7.729	6.389	4.408	5.813
$\delta(^{13}C)$(calcd)	129.4	129.4	129.3	129.2	129.1	129.3	131.4	131.7	131.0	132.2	132.1
std dev	0.66	0.40	0.44	0.51	0.48	0.48	0.60	0.48	0.38	0.47	0.56

[a] Distances are in angstroms. [b] Reference 5b. [c] Reference 5c. [d] Reference 5d. [e] Reference 5f. [f] Average force per bond in kcal/Å.

Table V. Calculated Geometry and ^{13}C NMR Shifts of Meta-Carbons (C_5, C_9) of Phenylethanes

compd	B	C	D	E	E'	F	G	G'	H	I	I'
C(o)-C(m) (found)[a]		1.390[b]				1.383[c]	1.386[d]	1.386		1.385[e]	1.386
C(o)-C(m) (calcd)	1.406	1.405	1.405	1.405	1.405	1.405	1.405	1.405	1.405	1.405	1.405
C(m)-C(p) (found)		1.370				1.366	1.373	1.369		1.376	1.370
C(m)-C(p) (calcd)	1.404	1.404	1.403	1.404	1.405	1.402	1.402	1.404	1.402	1.400	1.401
C(m)-H (found)						0.975	0.984	0.990		0.963	1.024
C(m)-H (calcd)	1.083	1.083	1.083	1.083	1.083	1.083	1.083	1.083	1.083	1.084	1.083
C(o)-C(m)-C(p) (found)		119.5				120.6	120.7	120.3		120.4	120.5
C(o)-C(m)-C(p) (calcd)	120.2	120.1	120.2	120.2	120.1	120.3	120.3	120.1	120.3	120.4	120.3
C(o)-C(m)-H (found)						117.6	119.2	119.6		119.0	116.1
C(o)-C(m)-H (calcd)	119.8	119.8	119.8	119.8	119.9	119.7	119.7	119.8	119.6	119.5	119.5
C(p)-C(m)-H (found)						121.8	120.2	120.2		121.7	123.3
C(p)-C(m)-H (calcd)	120.0	120.0	120.0	120.0	120.1	120.1	120.1	120.0	120.1	120.1	120.1
force $C(sp^2)$-H[f]	−9.88	−9.78	−9.79	−9.66	−9.69	−9.82	−9.82	−9.63	−10.1	−10.1	−10.1
force $C(sp^2)$-$C(sp^2)$	7.625	8.084	6.646	6.932	8.304	4.653	4.132	8.035	5.227	3.005	5.092
$\delta(^{13}C)$(calcd)	129.5	129.4	129.5	129.2	129.2	129.0	128.4	128.6	128.8	128.3	128.7
std dev	0.21	0.12	0.14	0.15	0.13	0.15	0.18	0.20	0.13	0.16	0.17

[a] Distances are in angstroms. [b] Reference 5b. [c] Reference 5c. [d] Reference 5d. [e] Reference 5f. [f] Average force per bond in kcal/Å.

steps at which time the net force on any particular atom was less than 0.1 kcal/Å (i.e., computationally zero). The geometries so obtained are reported in Tables II–VI where the experimentally obtained values are presented just above the calculated ones for comparison purposes. Thus with increasing phenyl substitution: (1) the ethane C(α)–C′(α) bond distances increases, (2) the C(α)–C(ipso) (i.e., C–Ph) bond distance increases, (3) the C(α)–C′(α)–H bond angle decreases, (4) the Ph–C(α)–C′(α) bond angle increases, (5) the H–C(α)–H bond angle decreases, (6) the Ph–C(α)–Ph bond angle remains nearly tetrahedral, (7) the average dihedral angle remains nearly 60°, which is what is expected for a staggered arrangement, (8) the C(ipso)–C(ortho) bond distance increases, (9) the C(α)–C(ipso)–C(ortho) bond angle increases, (10) the C(ortho)–C(ipso)–C′(ortho) bond angle increases, and (11) there is a slight opening of the C(ipso)–C(ortho)–C(meta) angle.

Although the same trends are reproduced in the calculated values as the X-ray structure derived quantities, the carbon–carbon

Table VI. Calculated Geometry of Para-Carbons (C_6, C_{10}) of Phenylethanes

compd	B	C	D	E	E'	F	G	G'	H	I	I'
C(m)-C(p) (found)[a]		1.375[b]				1.366[c]	1.373[d]	1.369		1.373[e]	1.370
C(m)-C(p) (calcd)	1.404	1.404	1.403	1.404	1.404	1.402	1.402	1.404	1.402	1.400	1.401
C(p)-H (found)						0.966	0.992	0.976		0.973	0.981
C(p)-H (calcd)	1.083	1.083	1.083	1.083	1.083	1.083	1.083	1.083	1.083	1.083	1.083
C(m)-C(p)-C(m') (found)		120.5				121.4	121.3	121.1		121.4	121.6
C(m)-C(p)-C(m') (calcd)	119.7	119.8	119.7	119.8	119.9	119.6	119.5	119.8	119.4	119.2	119.3
C(m)-C(p)-H (found)						120.3	120.5	120.1		120.4	120.4
C(m)-C(p)-H (calcd)	120.1	120.1	120.1	120.1	120.1	120.2	120.2	120.1	120.2	120.4	120.3
force $C(sp^2)$-H[f]	-8.80	-8.99	-8.64	-8.68	-9.00	-8.13	-7.92	-8.77	-8.01	-7.44	-7.75
force $C(sp^2)$-$C(sp^2)$	9.780	9.844	9.776	9.783	9.935	9.663	9.633	9.882	9.700	9.576	9.674

[a] Distances are in angstroms. [b] Reference 5b. [c] Reference 5c. [d] Reference 5d. [e] Reference 5f. [f] Average force per bond in kcal/Å.

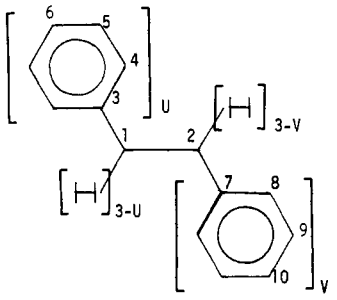

Compound	Letter Disignation	U	V
Ethane	A	0	0
Ethylbenzene	B	1	0
1,2 Diphenylethane	C	1	1
1,1 Diphenylethane	D	2	0
1,1,2 Triphenylethane	E	2	1
1,1,1 Triphenylethane	F	3	0
1,1,1,2 Tetraphenylethane	G	3	1
1,1,2,2 Tetraphenylethane	H	2	2
1,1,1,2,2 Pentaphenylethane	I	3	2

Figure 1.

bond lengths deviate as much as 0.03 Å. Although these differences are significant they are not larger than what has been found by using QCFF/PI + MCA calculations on other related systems.[18] Furthermore, since we are interested only in the nonbonding force on each atom, it is of no particular significance whether the value of an individual bond length is reproduced but that it should change with the same pattern (as its experimentally found counterpart) as the result of a change in force on that bond. In order to quantize the van der Waals forces on the atoms, we evaluated the components of the nonbonded forces along the bonds surrounding any particular atom in the following manner.

The QCFF/PI + MCA program automatically calculates the total force vector on each atom. At the calculated relaxed geometry the total force on each atom is zero, as a result of the nonbonded forces being exactly balanced by the opposing forces from all other contributors (e.g., bending and stretching). Thus, the nonbonded forces on each atom were calculated directly, using the QCFF/PI + MCA program, by evaluating the force vector at the relaxed geometry while skipping all potential functions except those for the nonbonded interactions.[20] The nonbonded force vector on each atom is then projected along the bonds by using eq 1–3, where

$$f(\mathrm{AB}) = f(\mathrm{A}) \cos\theta(\mathrm{A}) - f(\mathrm{B}) \cos\theta(\mathrm{B}) \quad (1)$$

$$\cos\theta(\mathrm{A}) = \mathbf{F}(\mathrm{A})\cdot\mathbf{R}(\mathrm{AB})/f(\mathrm{A})r(\mathrm{AB}) \quad (2)$$

$$\cos\theta(\mathrm{B}) = \mathbf{F}(\mathrm{B})\cdot\mathbf{R}(\mathrm{AB})/f(\mathrm{A})r(\mathrm{AB}) \quad (3)$$

f(AB) = the total nonbonded force along the bond between atoms A and B, f(A) = the magnitude of the nonbonded force on A, f(B) = the magnitude of the nonbonded force on B, **F**(A) = the nonbonded vector force on A, **F**(B) = the nonbonded vector force on B, θ(A) = the angle between the bond vector **R**(AB) and the nonbonded force vector **F**(A), θ(B) = the angle between the bond vector **R**(AB) and the nonbonded force vector **F**(B), **R**(AB) = the bond vector between atoms A and B, and r(AB) = the magnitude of the bond vector. The sign of the force, f(AB), is determined by the way the bond vector is defined. Throughout this paper a compressional force has a negative sign and a stretching force a positive sign.

The Grant–Cheney treatment ascribes the effect of van der Waals interactions on the γ substituent parameter to sterically induced charge polarization along the involved bonds. Assuming this mechanism to be valid and with the added dimension of both atoms experiencing nonbonded interactions, we have no reason to expect the amount of charge polarization per unit force or the direction of the dipole thereby induced along a bond to be the same for bonds of different hybridization or location in the molecule. Therefore, we have set up the equations of regression, eq 4–7, accordingly,

α-carbons

$$\delta(^{13}\mathrm{C}) = bm + cn + dF(\mathrm{C(sp^3)\text{–}H}) + eF(\mathrm{C(sp^3)\text{–}C(sp^3)}) + fF(\mathrm{C(sp^3)\text{–}C(sp^2)}) + r \quad (4)$$

ipso-carbons

$$\delta(^{13}\mathrm{C}) = b(m-1) + cn + fF(\mathrm{C(sp^3)\text{–}C(sp^2)}) + gF(\mathrm{C(sp^2)\text{–}C(sp^2)}) + r \quad (5)$$

ortho-carbons

$$\delta(^{13}\mathrm{C}) = b(m-1) + cn + gF(\mathrm{C(sp^2)\text{–}C(sp^2)}) + hF(\mathrm{C(sp^2)\text{–}H})) + r \quad (6)$$

meta-carbons

$$\delta(^{13}\mathrm{C}) = b(m-1) + cn + gF(\mathrm{C(sp^2)\text{–}C(sp^2)}) + hF(\mathrm{C(sp^2)\text{–}H})) + r \quad (7)$$

$\delta(^{13}\mathrm{C})$ = the observed ^{13}C NMR shift, m = the substituent parameter (vide infra), n = the substituent parameter (vide infra), $F(\mathrm{C(sp^3)\text{–}H})$ = the sum of the force along all carbon(sp^3)–hydrogen bonds (in kcal/Å) attached to the particular position being considered, $F(\mathrm{C(sp^3)\text{–}C(sp^3)})$ = the sum of the force along all carbon(sp^3)–carbon(sp^3) bonds in kcal/Å attached to the particular position being examined, $F(\mathrm{C(sp^3)\text{–}C(sp^2)})$ = the sum of the force along all carbon(sp^3)–carbon(sp^2) bonds (in kcal/Å) attached to the particular position being examined, $F(\mathrm{C(sp^2)\text{–}C(sp^2)})$ = the sum of the force along all carbon(sp^2)–carbon(sp^2) bonds (in kcal/Å) attached to the particular position being examined, $F(\mathrm{C(sp^2)\text{–}H})$ = the sum of the force along all carbon(sp^2)–hydrogen bonds (in kcal/Å) attached to the particular position being examined, b, c, d, e, f, g and h = the coefficients resulting from the multiple regression of the above defined independent variables with the observed ^{13}C shift as the dependent variable, and r = the intercept of the $\delta(^{13}\mathrm{C})$ axis.

The results of the multiple regression are presented in Table VII; the regressions were performed by using the MINITAB II program.[21] As one can see from the overall correlation coefficient

(20) The relevant sections of the QCFF/PI + MCA program that were skipped by the insertion of appropriate fortran statements were BONDP, REPULS, THETAP, and PHIP leaving only NONBON to contribute to the calculated force vectors, see ref 18b for a further discussion of the role these sections play.

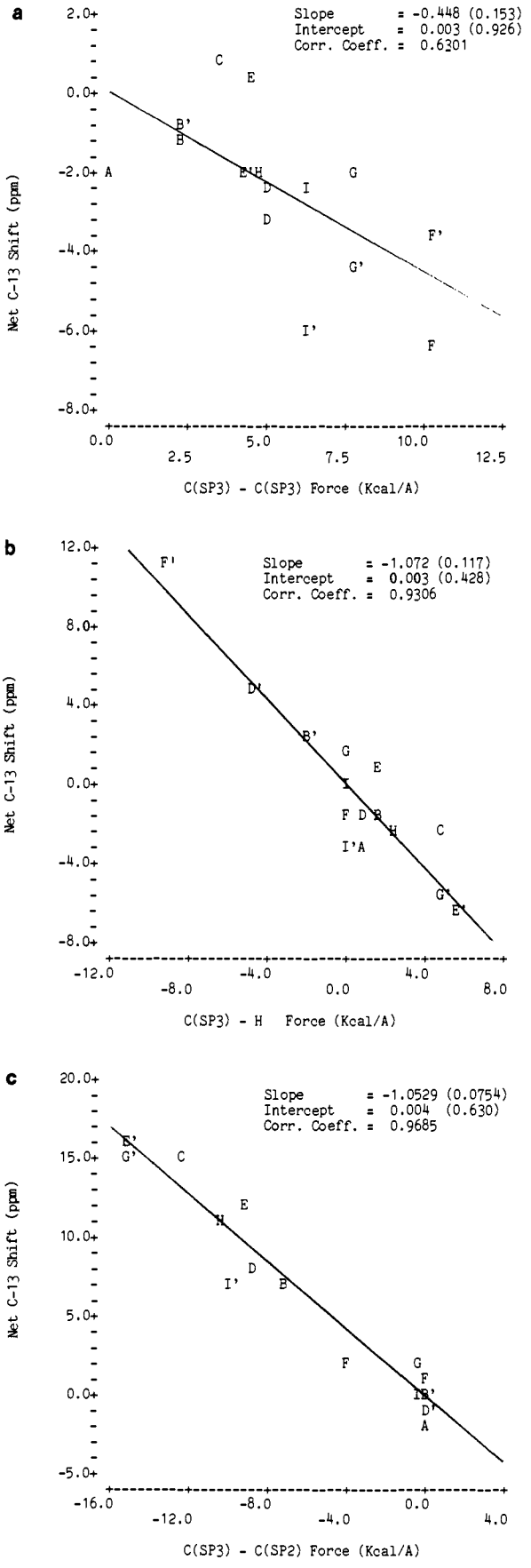

Figure 2. (a) Plot of the net ^{13}C shift for the α-carbons vs. the nonbonding force along the C(α)–C′(α) bond. The numbers in parentheses are standard deviations. (b) Plot of the net ^{13}C shift for the α-carbons vs. the nonbonding force along the C(α)–H bond. (c) Plot of the net ^{13}C shift for the α-carbons vs. the nonbonding force along the C(α)–C(ipso) bond.

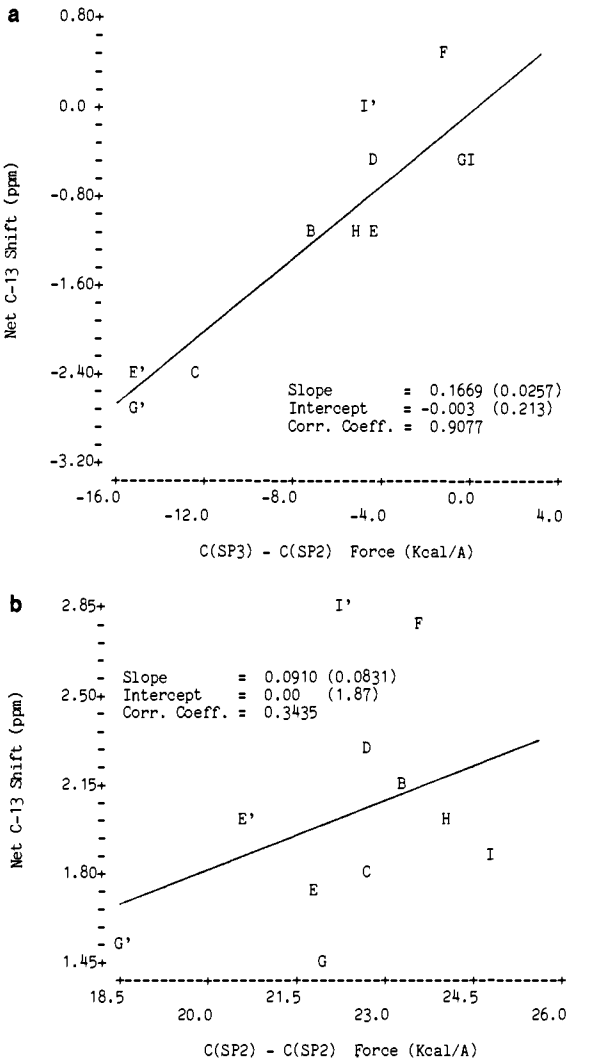

Figure 3. (a) Plot of the net ^{13}C shift for the ipso-carbons vs. the nonbonding force along the C(α)–C(ipso) bond. (b) Plot of the net ^{13}C shift for the ipso-carbons vs. the nonbonding force along the C(ipso)–C(ortho) bond.

and standard deviation in the dependent variable $\delta(^{13}C)$ about the regression line, the data are accounted for reasonably well by the model. Also, in Tables II–IV are contained the calculated ^{13}C NMR shifts and their standard deviations. Figures 2 through 5 contain plots of the component of the ^{13}C shift due to a particular force vs. the value of that force. This "net ^{13}C shift" is calculated by solving eq 4–7 for each term containing a force. An example is as follows

$$\delta(^{13}C) - [b(m-1) + cn + gF(C(sp^2)\text{–}C(sp^2))] = hF(C(sp^2)\text{–}H) \quad (8)$$

A plot of the left-hand side of eq 8 vs. $F(C(sp^2)\text{–}H)$ is contained in Figure 5a along with the slope, y intercept, and correlation coefficient. The letters used in the plots are the same as those defined in Figure 1. These figures illustrate the effect that the van der Waals interactions are having on the overall ^{13}C shift. Figure 2a shows how the nonbonded stretching force on the C_1–C_2 bond causes an upfield shift of these carbons. Unlike Figure 2a where for all of the compounds the force is positive (i.e., stretching), Figure 2b shows that the hydrogens attached to C_2 in 1,1,1-triphenylethane (F′) are compressed toward the carbon producing a deshielding of 11.0 ppm while the same hydrogens in 1,1,2-triphenylethane (E′) are being stretched away from C_2

(21) Ryan, T. A.; Joiner, B. L.; Ryan, B. F. "Minitab: Student Handbook"; Duxbury Press: New York, 1976.

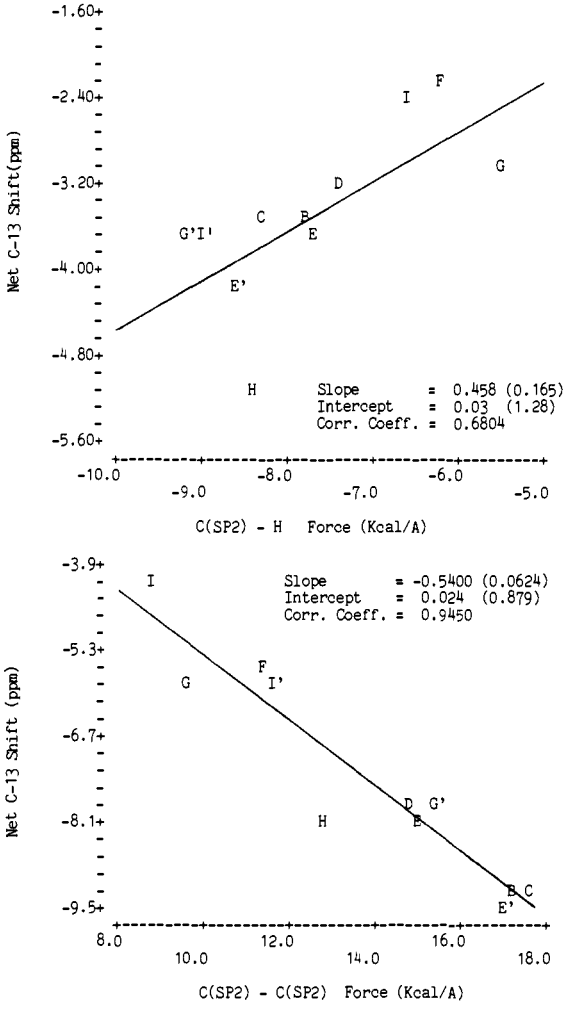

Figure 4. (a) Plot of the net ^{13}C shift for the ortho-carbons vs. the nonbonding force along the C(ortho)–H bond. (b) Plot of the net ^{13}C shift for the ortho-carbons vs. the nonbonding force along the C(ortho)–C(ipso) plus C(ortho)–C(meta) bonds.

producing a shielding of –6.1 ppm. The two plots describing the ipso-carbons' reaction to nonbonded interactions are presented in parts a and b of Figure 3. While Figure 3a exhibits a reasonably good correlation with the C(sp^3)–C(sp^2) force, Figure 3b shows little correlation with the total C(sp^2)–C(sp^2) force. What is not immediately obvious, however, is that the standard deviation of y (i.e., the net ^{13}C shift) about the regression line is the same for the two plots (which is an inherent property of the least-squares procedure). Thus further investigation of compounds where the C(sp^2)–C(sp^2) force of the ipso-carbon covers a larger range of values is needed before any conclusions can be drawn concerning the seemingly poor fit of Figure 3b. Parts a and b of Figure 4 and parts a and b of Figure 5 are plots for the ortho and meta positions and show a moderately good correlation with their forces. It is these plots, particularly the ones involving the C(sp^2)–H bonds which should show a considerable amount of deviation from linearity if the C_1–C_2 dihedral angle (Table II) and ring twist angle (Table III) were major contributors to the nonbonding force. Mislow et al.[4] have found the difference in energy between various conformations of these compounds to be small, and therefore it is none too surprising that where the calculated angles do not match the experimental values, this difference is not reflected significantly in the nonbonding forces.

The numbers in parentheses in Figures 2 through 5 are the standard deviations. If the variables were perfectly independent of one another the standard deviations should be the same as those reported in Table VII after an adjustment for the number of degrees of freedom (multiply the standard deviations of parts a, b, and c of Figure 3 by 1.20 and parts a and b of Figure 3, parts a and b of Figure 4, and parts a and b of Figure 5 by 1.22). The reason for this discrepancy is what is referred to as multicollinearity,[22] that is, the "independent" variables are related to one another. The degree of collinearity of the variables has been

Table VII. Results of Multiple Regression

	α	ipso	ortho	meta
substituent parameter (b)	15.353	1.585	−1.71	1.289
	(0.757)[a]	(0.583)	(1.410)	(0.730)
	[1.000][b]	[0.982]	[0.824]	[0.936]
substituent parameter (c)	5.118	−1.281	0.852	−0.129
	(0.621)	(0.184)	(0.539)	(0.101)
	[1.000]	[1.000]	[0.914]	[0.875]
force [C(sp^3)-H] (d)	−1.072			
	(0.345)			
	[0.994]			
force [C(sp^2)-C(sp^3)] (f)	−1.053	0.167		
	(0.188)	(0.105)		
	[1.000]	[0.919]		
force [C(sp^2)-H] (h)			0.456	−3.59
			(0.519)	(1.53)
			[0.793]	[0.971]
force [C(sp^3)-C(sp^3)] (e)	−0.448			
	(0.327)			
	[0.897]			
force [C(sp^2)-C(sp^2)] (g)		0.091	−0.539	0.477
		(0.157)	(0.390)	(0.205)
		[0.708]	[0.891]	[0.970]
R(i) [intercept]	9.85	144.35	141.68	86.8
	(1.32)	(4.21)	(7.27)	(18.2)
	[1.000]	[1.000]	[1.000]	[0.998]
correlation coeff	0.9960	0.9899	0.9220	0.9225
correlation coeff (corr.)[c]	0.9935	0.9834	0.8660	0.8672
degrees of freedom	9	6	6	6
std dev about regression line	1.98	0.55	0.75	0.24

[a] The numbers in parentheses are standard deviations. [b] The numbers in brackets are the probabilities the values are nonzero (i.e., the signs are correct). [c] Corrected for the number of degrees of freedom.

Table VIII. Correlation Coefficients of Variables

α

	M	N	E	D	F
M	1.00000	−0.13636	0.43920	0.29553	0.12176
N	−0.13636	1.00000	0.43920	−0.18898	0.25390
E	0.43920	0.43920	1.00000	−0.33450	−0.04829
D	0.29553	−0.18898	−0.33450	1.00000	0.76937
F	0.12176	0.25390	−0.04829	0.76937	1.00000

Ipso

	$M-1$	N	F	G
$M-1$	1.00000	−0.17576	0.91018	0.52937
N	−0.17576	1.00000	−0.36385	−0.42895
F	0.91018	−0.36385	1.00000	0.70651
G	0.52937	−0.42895	0.70651	1.00000

Ortho

	$M-1$	N	H	G
$M-1$	1.00000	−0.17576	0.79228	−0.92064
N	−0.17576	1.00000	−0.59064	−0.16624
H	0.79228	−0.59064	1.00000	−0.59824
G	−0.92064	−0.16624	−0.59824	1.00000

Meta

	$M-1$	N	H	G
$M-1$	1.00000	−0.17576	−0.44179	−0.93182
N	−0.17576	1.00000	−0.21374	−0.03751
H	−0.44179	−0.21374	1.00000	0.71161
G	−0.93182	−0.03751	0.71161	1.00000

(22) Beaton, A. E.; Tukey, J. W. *Technometrics* **1974**, *16*, 147–192.

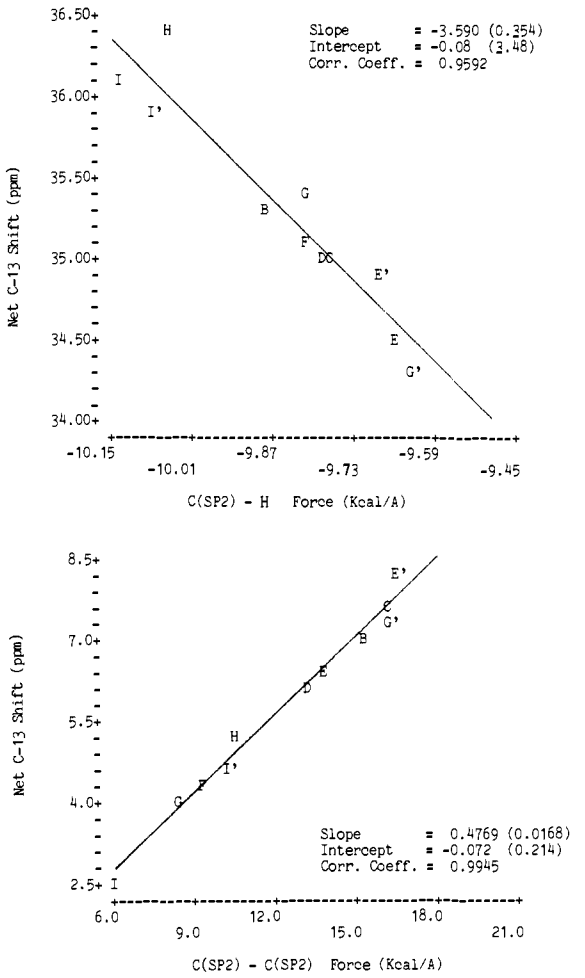

Figure 5. (a) Plot of the net ^{13}C shift for the meta-carbons vs. the nonbonding force along the C(meta)–H bond. (b) Plot of the net ^{13}C shift for the meta-carbon vs. the nonbonding force along the C(meta)–C(ortho) plus C(meta)–C(para) bonds.

ascertained by performing a regression of one variable against the other,[23] the results of which are presented in Table VIII. While we did not expect this complication, in hindsight its presence is not too surprising. What Table VIII is telling us, for example, is that for the force along meta's sp^2–sp^2 bonds changes in the same manner as that of the substituent parameter (m – 1). Therefore, in our discussion of the results we have limited ourselves to interpretations which rely only on the sign of the coefficients. The probability that the signs are well-founded are based upon the t ratio[24] and are presented in Table VII. The only assumption that is implicit in the model is that the carbon-shielding response to a force applied along similar bonds attached to a particular carbon is the same. By way of example let us examine the case of the ortho-carbon in order to demonstrate the way this assumption operates in the model equations. The ortho-carbon is attached to two other aromatic carbons, ipso and meta, and the model assumes that a force along the ipso–ortho bond will affect the NMR shift in an identical manner as when that same force is applied along the ortho–meta bond. While the data were not sufficient to test this approximation explicitly, we point to the linearity of the plots of the ortho- and meta-carbon's sp^2–sp^2 force vs. the net ^{13}C shift (Figures 4b and 5b) to support the validity of this premise.

(23) These correlations were performed by using the following statistics package: Nie, N. H.; Hull, C. H.; Jenkins, J. G.; Steinbrenner, K.; Bent, D. H. "SPSS: Statistical Package for the Social Sciences"; McGraw-Hill: New York, 1975.

(24) Burington, R. S.; May, D. C. "Handbook of Probability and Statistics with Tables"; Handbook Publishers Inc.: New York, 1953; pp 283–285.

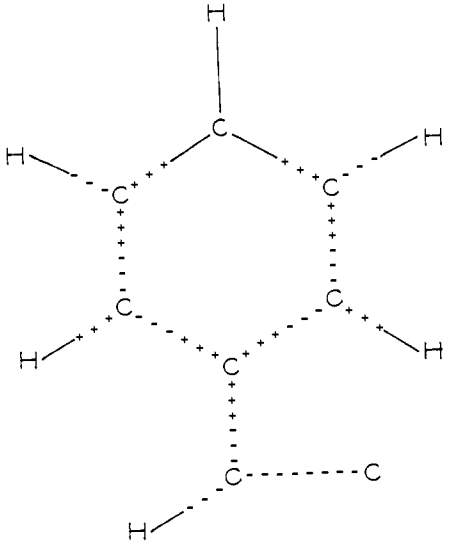

Figure 6. Diagram showing polarization of electrons: (+) indicates positive coefficient; (–) indicates negative coefficient.

Discussion

Clearly further work with a larger data set and encompassing other types of organic compounds needs to be done before this approach can be used as a predictive tool. However, certain conclusions can be inferred from the following observations. First, the ^{13}C NMR shift of the aromatic carbons do not respond the same to forces along their attached bonds. For instance, both ortho and meta are aromatic carbons bonded to two other aromatic carbons and one hydrogen. If a compressive force (i.e., a force less than zero) is applied to their C–H bonds, the ortho-carbon is shielded while the meta-carbon is deshielded. Similarly, if that same force is employed along their C–C bonds, the ortho-carbon is deshielded while the meta-carbon is shielded. Second, carbons subtending the same bond respond differently to a force applied along that bond. The α- and ipso-carbons in 1,2-diphenylethane illustrate this point: the force along their common bond is –12.2 kcal/Å (compressive); this is calculated to cause a contribution of +12.9 ppm (i.e., deshielding) to the α-carbon and –2.0 ppm (i.e., shielding) to the ipso-carbon. Third, a map of the sign of the ^{13}C shift response to nonbonding forces (i.e., the signs of the coefficients of the forces employed in the multiple regression) exhibits an alternation in sign along each bond (see Figure 6). In Grant and Cheney's treatment they ascribed the effect of nonbonded interactions to Coulombic repulsion between the valence electrons of the hydrogens attached to the γ-carbon with that of the hydrogens of the substituent placed on the α-carbon which in turn caused electron density to shift away from hydrogen toward carbon [i.e., C(δ–)—H(δ+)] and thus produced an upfield shift of the ^{13}C NMR signal because of the increase in electron density. In the present approach both atoms which subtend the bond being acted upon are presumed to be encountering van der Waals interactions with other atoms in the molecule, and therefore it is not clear which direction the electrons should be polarized. The above situation described by Grant and Cheney is considered in the present model as a compression (i.e., a force less than zero) of the C–H bond. But an examination of Figures 2b, 4a, and 5a reveals that a compressive force along C–H bonds produces a deshielding effect for the α- and meta-carbons and a shielding effect for the ortho-carbon, contrary to what would have been predicted by the earlier model. Of course we are no longer considering only γ H···H interactions but all nonbonded interactions on all atoms along their common bond. With these basic differences in mind the central theme of their model still remains, that is, that a polarization of electrons along a bond is induced by nonbonded interactions. While it had not been possible to experimentally substantiate this previously, with the more general approach presented here, considerable evidence points to the fact that this is indeed the case, as is evidenced by Figure 6. Here,

the effect of nonbonded interactions on the ^{13}C shift along each bond of each position is pictorially represented by placing "+" where the corresponding coefficient from the multiple regression is positive and a "-" where it is negative. Unfortunately, it will have to await further study before any predictive rules can be developed as to which direction these induced dipoles will take in more general cases. We have stated earlier (vide infra) that the para-carbon shift remains unchanged throughout this series of compounds. If these ^{13}C shifts are due to charge polarization brought on by van der Waals interactions, then the lack of change in the para-carbon shift indicates that the π system is unaffected and that the polarization occurs solely in the σ system. For instance, the calculated net ^{13}C shift for C_4 of pentaphenylethane due to nonbonding forces along its bonds is -7.75 ppm, and for 1,2-diphenylethane this value is -13.29 ppm. Thus in going from 1,2-diphenylethane to pentaphenylethane the ortho-carbon (C_4) is shifted downfield by 5.54 ppm due to the change in nonbonding interactions in these two molecules. If this downfield shift is due to an accumulation of positive charge on the ortho carbons, then simple resonance theory[25] tells us that a similar amount of positive charge should buildup on the para-carbon and thus we would expect a downfield shift of its ^{13}C signal. Theory[25] further tells us that, to a first approximation, the σ and π systems of an aromatic ring are independent of one another. Thus it would appear the polarization of electrons is perturbing only the σ-electron distribution and not significantly effecting the π electrons. One exception to the observed sign alternation is the α-α' bond. Here a stretching force causes an upfield shift of both tetrahedral carbons. This is a consequence of the symmetry of these compounds; thus if 1,1,2,2-tetraphenylethane were stretched along the α-α' bond, a dipole is not expected to be produced since the two carbons are by symmetry the same. In a previous paper[26] we had endeavored to correlate the ^{13}C shift of α-substituted benzyl cations with calculated (CNDO/2) charge densities. While the ^{13}C shifts of the para position lay close to the least-squares line ($r = 0.980$), the shifts for the other positions deviated considerably. One possible reason now offers itself: the electron densities of the α, ipso, ortho, and meta positions conceivably are altered by van der Waals interactions within the molecule, an effect which is not dealt with explicitly at the CNDO/2 level.

In summary we have shown (1) the induced polarization of electrons along each bond by steric interactions previously postulated by Grant and Cheney, (2) that van der Waals interactions are equally important for all positions, and (3) a general treatment for elucidating steric effects in organic compounds using ^{13}C NMR. Our primary purpose here has not been to reproduce experimentally found ^{13}C shifts but to ferret out one of the factors that determines them. It is hoped that ultimately a model will be devised in which a term as vague as a "substituent effect" can be eliminated and replaced with one reflecting the change in the electronic properties induced in a molecule by the substituents and thus make it possible to have a model based on experimental observations as interpreted by theory to predict the electronic as well as steric properties of a molecule.

Experimental Section

^{13}C Spectroscopy. The study was carried out by using a Varian Associates Model XL-200 spectrometer; the instrument and techniques used are analogous to those described previously for the XL-100.[27] All reported shifts are at ambient temperature in $CDCl_3$ (0.5 M) and are referenced to external capillary tetramethylsilane.

Preparation of Phenylethanes. 1,1,1,2,2-Pentaphenylethane was prepared according to the method of Bachmann.[28] The purification was modified by washing the crude product with diethyl ether before recrystallization. The yield was 85.7%; mp 180 °C (lit. 182-185 °C). Anal. Calcd: C, 93.65; H, 6.34. Found: C, 93.77; H, 6.21. 1,1,1,2-Tetraphenylethane was prepared by the procedure of Bachmann and Cockerill,[29] with a yield of 83.4%; mp 142 °C (lit.[30] 143.6 °C). 1,1,1-Triphenylethane was also synthesized by the method of Bachmann,[29] the yield was 93.2%; mp 94 °C (lit.[28] 94.9 °C). All other compounds were commercially available and used without further purification.

Acknowledgment. We gratefully acknowledge the National Science Foundation for financial support of this work and Professor A. Warshel and Professor F. A. L. Anet for many helpful discussions.

(25) Dewar, M. J. S. "The Molecular Orbital Theory of Organic Chemistry"; McGraw-Hill: New York, 1969; pp 153-190.
(26) Olah, G. A.; Westerman, P. W.; Forsyth, D. A. *J. Am. Chem. Soc.* **1975**, *97*, 3419-3427.
(27) Olah, G. A.; Liang, G.; Westerman, P. *J. Am. Chem. Soc.* **1973**, *95*, 3698-3705.
(28) Bachmann, W. E. *J. Am. Chem. Soc.* **1933**, *55*, 2135-2139.
(29) Bachmann, W. E.; Cockerill, R. F. *J. Am. Chem. Soc.* **1933**, *55*, 2932-2941.
(30) Smith, R. H.; Andrews, D. H. *J. Am. Chem. Soc.* **1931**, *53*, 3644-3660.

Proton Nuclear Overhauser Effects and Protein Dynamics

E. T. Olejniczak, F. M. Poulsen, and C. M. Dobson*

Contribution from the Department of Chemistry, Harvard University, Cambridge, Massachusetts 02138. *Received January 26, 1981*

Abstract: The rates of direct nuclear cross-relaxation between pairs of protons of three amino acid residues of hen lysozyme (Trp-28, Ile-98, and Met-105) have been obtained at 270 and 498 MHz by analyzing the time dependence of nuclear Overhauser effects. The proton pairs were chosen to have short internuclear distances fixed by the geometry of the residues themselves. The measured cross-relaxation rates were compared with rates calculated on the assumption that the protein molecule behaves as a rigid body tumbling isotropically in solution with a rotational correlation time defined from independent studies. Differences between the measured and calculated rates were attributed to the effects of significant internal motions. It was demonstrated that the proton cross-relaxation data can define the extent of specific types of internal motion. As an example, limits were placed on the magnitude of subnanosecond fluctuations of individual side-chain torsional angles by using a restricted diffusion model. The consequences of the experiments for investigation of molecular dynamics, for structural studies, and for other relaxation phenomena are discussed.

Saturation of a specific resonance in the nuclear magnetic resonance spectrum of a molecule can give rise to changes in the intensities of other resonances through the nuclear Overhauser effect.[1] In a system of dipolar coupled spins, the magnitude of the effect on a given spin following saturation of another for a fixed length of time depends on the frequencies of the motions

*To whom correspondence should be addressed at the Inorganic Chemistry Laboratory, South Parks Road, Oxford OX1 3QR, England.

(1) J. H. Noggle and R. E. Shirmer "The Nuclear Overhauser Effect", Academic Press, New York, 1971.

0002-7863/81/1503-6574$01.25/0